Journal of Solid State Chemistry 182 (2009) 2252–2260

Contents lists available at ScienceDirect

Journal of Solid State Chemistry

journal homepage: www.elsevier.com/locate/jssc

First discovery and structural characterization of a new compound in Al–Si–O–C system

Tomoyuki Iwata [a], Motoaki Kaga [a], Hiromi Nakano [b], Koichiro Fukuda [a,*]

[a] Department of Environmental and Materials Engineering, Nagoya Institute of Technology, Nagoya 466-8555, Japan
[b] Electron Microscope Laboratory, Ryukoku University, Otsu 520-2194, Japan

ARTICLE INFO

Article history:
Received 15 April 2009
Received in revised form
2 June 2009
Accepted 7 June 2009
Available online 13 June 2009

Keywords:
Crystal structure
Powder diffraction
Rietveld method
New material
Oxycarbide

ABSTRACT

A quaternary oxycarbide, $[Al_{16.77(5)}Si_{1.23(5)}]_{\Sigma_{18}}[O_{3.04(9)}C_{10.96(9)}]_{\Sigma_{14}}$, has been for the first time discovered in the Al–Si–O–C system. The crystal structure was characterized by X-ray powder diffraction, transmission electron microscopy and energy dispersive X-ray spectroscopy (EDX). The atom ratios [Al:Si] were determined by EDX, and the initial structural model was derived by the direct methods. The structural parameters as well as the atom ratios [O:C] were determined by the Rietveld method. The crystal is monoclinic (space group $C2/m$, $Z=1$) with lattice dimensions $a=0.57404(1)$ nm, $b=0.331435(5)$ nm, $c=1.92410(2)$ nm, $\beta=90.036(1)^\circ$ and $V=0.366076(9)$ nm^3. The final structural model showed the positional disordering of Al/Si sites. The validity of the split-atom model was verified by the three-dimensional electron density distribution, the structural bias of which was reduced as much as possible using the maximum-entropy methods-based pattern fitting (MPF). The reliability indices calculated from the MPF were $R_{wp}=4.20\%$ ($S=1.14$), $R_p=3.09\%$, $R_B=0.92\%$ and $R_F=1.05\%$. The crystal was an inversion twin with nearly the same twin fraction.

1. Introduction

The binary and ternary carbides in the Al–Si–C system have the characteristics of layered structures [1–7]. The crystal structure of Al_4C_3 (space group $R\bar{3}m$, $Z=3$) is composed of an $[Al_2C_2]$ double layer of AlC_4 tetrahedra surrounded by two $[AlC_2]$ single layers of AlC_4 tetrahedra [2,3]. These three layers form an $[Al_4C_4]$ unit layer (A). The complete structure is the superposition of three A layers along the c axis, in which the layer stacking sequence is described by $\langle AAA \rangle$. There are five types of ternary carbides reported so far: Al_4SiC_4, $Al_4Si_2C_5$, $Al_4Si_3C_6$, $Al_4Si_4C_7$ and Al_8SiC_7 [1,4–7]. The crystal structures of the former two carbides have been determined by single crystal X-ray diffraction method [5]. The structure of Al_4SiC_4 ($P6_3mc$, $Z=2$) requires an additional $[(Al,Si)C_2]$ single layer (B) of $(Al,Si)C_4$ tetrahedra in the hexagonal lattice to be alternately inserted between the A-type $[(Al,Si)_4C_4]$ unit layers with stacking sequence of $\langle BABA \rangle$. With the rhombohedral lattice of $Al_4Si_2C_5$ ($R\bar{3}m$, $Z=3$), the stacking sequence is $\langle BABBABBAB \rangle$. Although crystal structures of $Al_4Si_3C_6$, $Al_4Si_4C_7$ and Al_8SiC_7 are still not elucidated, they could be made up of the combinations of A and B layers. Oscroft et al. have proposed the most probable stacking sequences in $Al_4Si_3C_6$ and $Al_4Si_4C_7$ [1]. Kidwell et al. have determined the hexagonal unit cell of $a=0.33127(7)$ nm and $c=1.9242(4)$ nm for Al_8SiC_7 [7].

In the Al–O–C system, two types of ternary oxycarbide compounds are known: Al_2OC [2,8–10] and Al_4O_4C [11,12]. The crystal structure of the former consists of mixed blocks described as $[AlO]_n[Al_2C_2]_n[AlO]_n$ with the C atoms in a similar environment to those in Al_4C_3 [2]. The structure of the latter can be described in terms of a three-dimensional network of $Al(O_3C)$ tetrahedra, which are associated by sharing edges and corners [12]. These crystal structures are distinct from those of the layered carbides in the Al–Si–C system. In the Al–Si–O–C system, quaternary compounds have never been recognized previously.

Recent advances in the field of crystal-structure analysis from X-ray powder diffraction (XRPD) data have enabled us to investigate unknown structures as well as disordered structures. To begin with initial structural models are required, which may be determined by, for example, direct methods [13]. The structural parameters are subsequently refined using the Rietveld method [14]. In order to disclose the structural details that had not been introduced into the structural models, the combined use of a maximum-entropy method (MEM) [15] and a MEM-based pattern fitting (MPF) method [16] is employed. MEM is capable of estimating structure factors of unobserved reflections and improving those of overlapped reflections, which give MEM advantages over the classical Fourier method. However, the Rietveld and MEM analyses are insufficient to readily determine charge densities because the observed structure factors, F_O (Rietveld), are

* Corresponding author.
E-mail address: fukuda.koichiro@nitech.ac.jp (K. Fukuda).

0022-4596/$ - see front matter © 2009 Elsevier Inc. All rights reserved.
doi:10.1016/j.jssc.2009.06.014

biased toward the structural model assuming intensity partitioning. The subsequent MPF method can minimize the structural bias. Thus, the MEM and MPF analyses are alternately repeated (REMEDY cycle) until the reliability indices reach minima. Crystal structures are represented not by structural parameters but by electron densities in MPF.

In the present study, we have for the first time discovered a new quaternary compound in the Al–Si–O–C system. We determined the initial structural model from XRPD data using direct methods and further modified it into a split-atom model, in which two of the five types of Al/Si sites were positionally disordered. The crystal is most probably an inversion twin with nearly the same twin fraction.

2. Experimental

2.1. Synthesis

The reagent-grade chemicals of Al (99.9%, KCL Co., Ltd., Saitama, Japan), Si (KCL, 99.99%) and C (graphite, KCL, 99.7%) were mixed in molar ratios of Al:Si:C = 11.2:1:7. The well-mixed chemicals were pressed into pellets ($\varnothing$ 15 mm × 10 mm), heated at 2273 K for 2 h in inert gas atmosphere of Ar, followed by cooling to ambient temperature by cutting furnace power. The reaction product was an aggregate of transparent platelet crystals with size up to 100 μm × 100 μm × 5 μm. The vaporization of Al and Si would significantly occur when melting at 2273 K, hence the crystals were most probably formed by a vapor-phase growth process.

2.2. Characterization

The crystals were finely ground to obtain powder specimen and subsequently introduced into a 0.5 mm diameter glass capillary tube of internal diameter approximately 0.3 mm. The XRPD intensities were collected on a diffractometer (X'Pert PRO MPD, PANalytical B.V., Almelo, The Netherlands) equipped with a high speed detector in Debye–Scherrer geometry using Cu$K\alpha$ radiation (45 kV, 40 mA) in a 2θ range from 1.9962° to 131.9931° (an accuracy in 2θ of ±0.0001°). Other experimental conditions were: continuous scan, total of 15 559 datapoints and total experimental time of 13.8 h. No preferred orientation could be seen in the diffraction pattern which was collected with the specimen rotating. We corrected the X-ray absorption using the μr value (μ: linear absorption coefficient; r: sample radius) of the sample and capillary tube, which was determined by the transmittance of direct incident beam. The structure data were standardized using the computer program STRUCTURE TIDY [17]. The crystal-structure models were visualized with the computer program VESTA [18].

The crushed fracture fragments were dispersed with air and deposited on a holey carbon film attached to a copper grid. They were examined using a transmission electron microscope (TEM) (JEM 3000F, JEOL Ltd., Tokyo, Japan) operated at 300 kV and equipped with an energy dispersive X-ray analyzer (EDX; VOYAGER III, NORAN Instruments, Middleton, WI, USA). Selected area electron diffraction (SAED) patterns and corresponding lattice images were obtained. A chemical analysis was made for nine crystal fragments to confirm the existence of O atoms within the crystal lattice as well as to quantitatively determine the atom ratios Al:Si. The correction was made by the ZAF routines.

3. Results and discussion

3.1. Crystal system, unit cell and chemical composition

Peak positions of the powder diffraction pattern were first determined using the computer program PowderX [19]. The 2θ

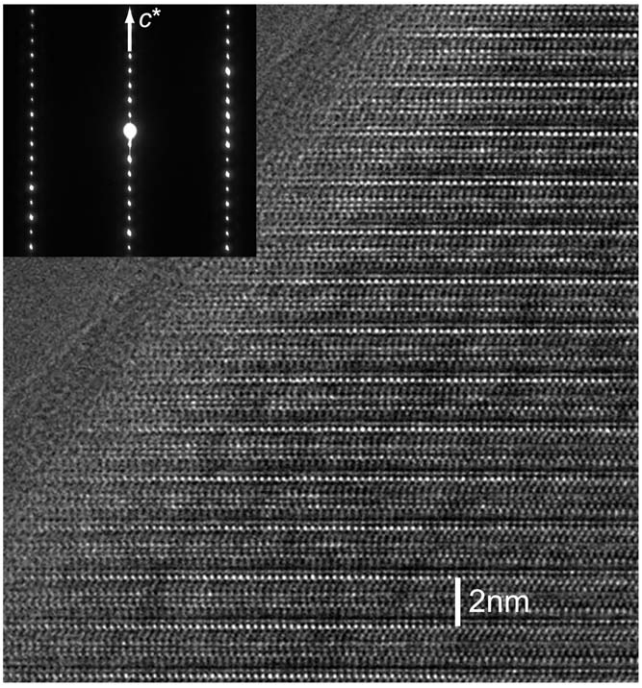

Fig. 1. Selected-area electron diffraction pattern and corresponding lattice image. Incident beam parallel to (001) plane.

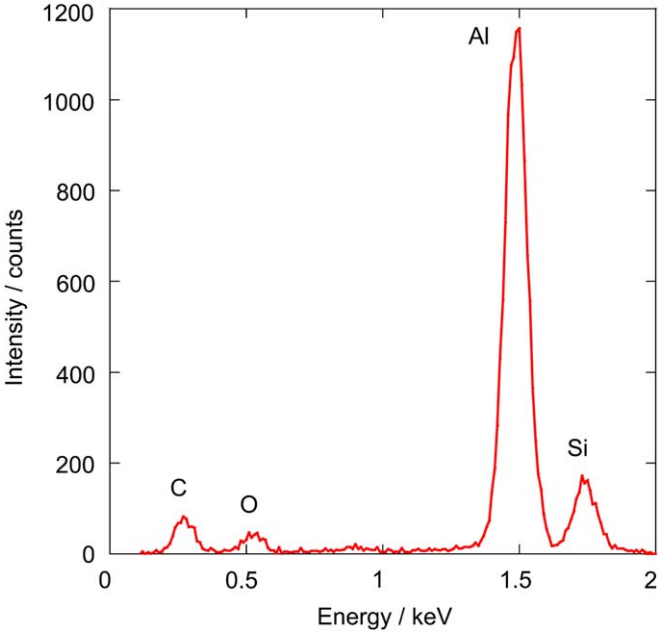

Fig. 2. Identification of the presence of Al, Si, O and C in the compound. EDX spectrum.

values of 20 observed peak positions within $2.0^\circ \leq 2\theta \leq 65.1^\circ$ were then used as input data to the automatic indexing computer program TREOR90 [20]. A hexagonal unit cell was found with satisfactory figures of merit $M_{20}/F_{20} = 54/37(0.016042, 34)$ [21,22]. The derived unit-cell dimensions of $a = 0.33180(3)$ nm and $c = 1.9270(3)$ nm were subsequently used as initial parameters

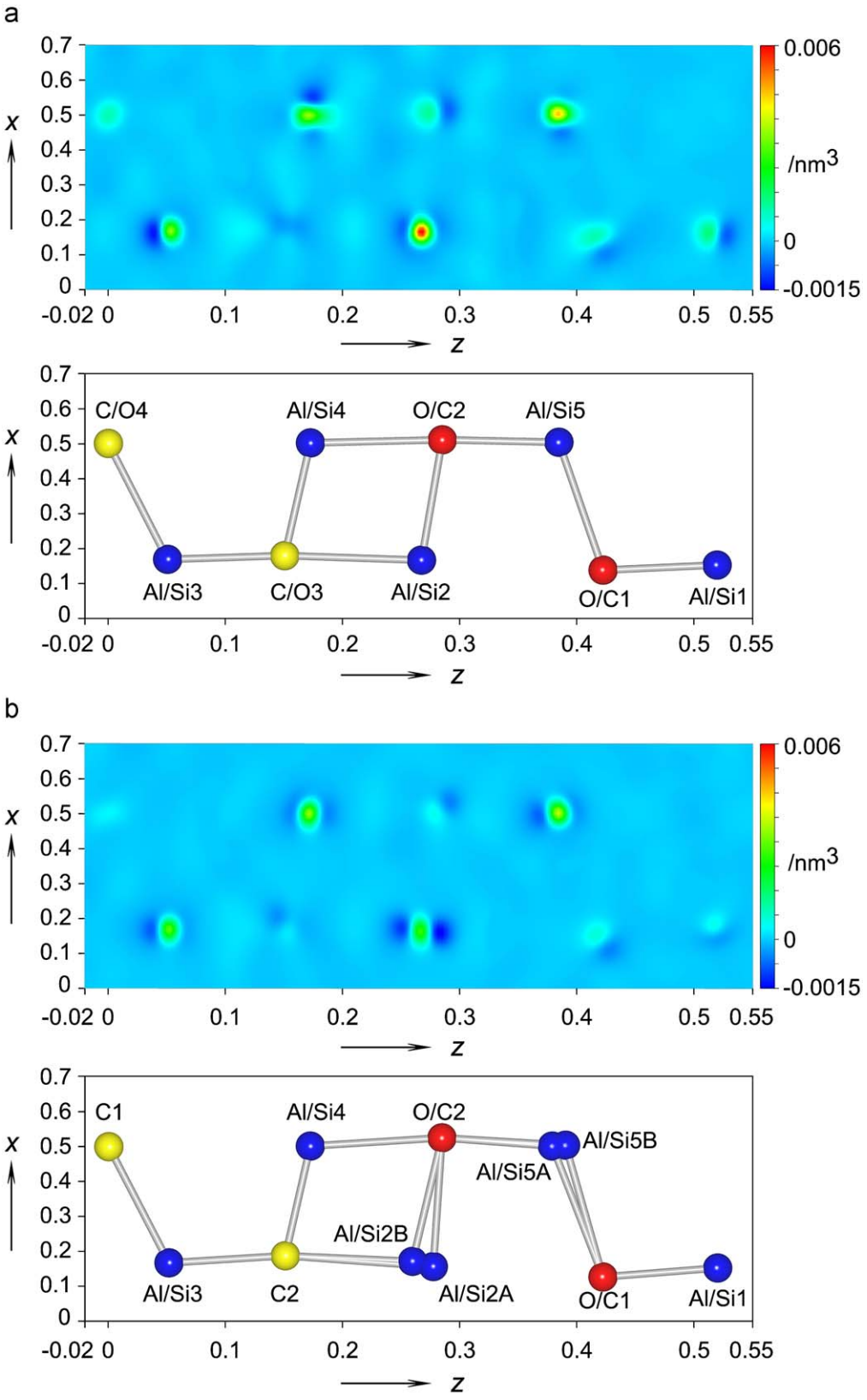

Fig. 3. Sections of electron-density-distribution difference with the plane $0 \leq x \leq 0.7$, $y = 0$, $-0.02 \leq z \leq 0.55$ (upper part), and the corresponding atomic configurations (lower part): (a) the initial model and (b) the split-atom model.

for the Le Bail method [23] using the computer program RIETAN-FP [24] in a wider 2θ range from 2.0° to 131.9°. However, the refinement was unsuccessful with relatively large reliability indices [25] of $R_{wp} = 5.97\%$ ($S = R_{wp}/R_e = 1.60$) and $R_p = 4.20\%$.

In subsequent Le Bail analysis, we assumed the crystal system to be monoclinic. The orthorhombic system is hardly expected for the crystal structure because it requires two-fold axes in three mutually perpendicular directions. The initial unit-cell dimensions used were $a = 0.57469$ nm, b ($= a/\sqrt{3}$) $= 0.33180$ nm, $c = 1.9270$ nm and $\beta = 90.0°$, which are comparable to those of the C-lattice orthohexagonal cell of the former hexagonal cell. The Le Bail analysis yielded much lower reliability indices of $R_{wp} = 4.17\%$ ($S = 1.13$) and $R_p = 3.06\%$. The refined unit-cell dimensions of $a = 0.57404(1)$ nm, $b = 0.331459(5)$ nm, $c = 1.92415(1)$ nm and $\beta = 90.033(1)°$ could successfully index all the observed reflections in the experimental diffraction pattern. The observed diffraction peaks were examined to determine the presence or absence of reflections. Systematic absences $h+k \neq 2n$ for $h\,k\,l$, $h \neq 2n$ for $h\,0\,l$ and $k \neq 2n$ for $0\,k\,0$ reflections were found, which implies that possible space groups are $C2$, Cm and $C2/m$.

The SAED pattern and corresponding lattice image (Fig. 1) indicate that the crystal is characterized by a layered structure with the periodicity of about 2 nm along the c axis. The EDX spectrum showed the existence of a small amount of O atoms within the crystal lattice (Fig. 2). The O atoms might be originated from the impurities of Ar gas and introduced into the sample during the crystal growth process. The atom ratios Al:Si were determined to be 0.932(3):0.068(3), where the numbers in parentheses indicate standard deviations. Accordingly, the present specimen must be a new compound which has been discovered for the first time in the Al–Si–O–C system. The unit cell was pseudohexagonal and compatible with that of Al_8SiC_7 ($V = 0.18287$ nm^3 and $Z = 1$) [7]. Because the unit-cell content of this compound is [8Al 1Si 7C] (Al+Si = 9), that of the new one ($V = 0.36611$ nm^3) must be [16.77Al 1.23Si 14(O+C)] (Al:Si = 0.932:0.068, Al+Si = 18), assuming that the O atoms exclusively occupy the C sites.

3.2. Initial structural model

Because the atomic scattering factors for Al and Si are almost the same and the oxygen concentration is relatively low, we used a unit-cell content with [18Al 14C] as input data for the search of a crystal-structure model. All of the possible space groups were tested using the EXPO2004 package [13] for crystal structure determination. A promising structural model with a minimum reliability index R_F of 7.88% was found with the space group $C2/m$ (centrosymmetric) in a default run of the program. There were nine independent sites in the unit cell; five Al/Si sites (Al/Si1, Al/Si2, Al/Si3, Al/Si4 and Al/Si5) and three O/C sites (O/C1, O/C2 and O/C3) were located at the Wyckoff position 4i, and one O/C site (O/C4) was located at 2b. The unit-cell content of this structural model was found to be [20Al 14C], suggesting that one of the site occupancies (g) of Al/Si sites should be reduced to one-half its initial value. The Al/Si1 sites were unusually close to each other with the distance of 0.189 nm, hence the g(Al/Si1)-value was reduced to 1/2. This implies that the crystal is twinned, the twin domains of which are related by a pseudo-symmetry inversion. The twinning structure of this compound will be discussed in more detail for the final structural model.

The structural parameters and unit-cell dimensions were refined by the Rietveld method using the computer program RIETAN-FP [24]. The chemical species (oxidation states) of Al, Si, O and C were adopted in the Rietveld analysis. A Legendre polynomial was fitted to background intensities with 12 adjustable parameters. The pseudo-Voigt function [26] was used to fit the peak profile. The occupancies of O and C atoms in each O/C site were refined without any constraints. The isotropic displacement (B) parameters for O and C atoms were constrained to be equal. Because the g and corresponding B parameters were strongly correlated, they were refined alternately in successive least-squares cycles. The O atoms preferentially occupied the O/C1 and O/C2 sites, the g(O)-values of which were 0.52(2) and 0.30(1), respectively. Because of the absence of O atoms at both O/C3 and O/C4 sites, they were relabeled C2 and C1, respectively. The refinement, however, resulted in unsatisfactory large R indices of $R_{wp} = 4.86\%$ ($S = 1.32$), $R_p = 3.53\%$, $R_B = 4.21\%$ and $R_F = 3.13\%$.

We expected MPF to enable us to extract structural details that had not been introduced into the initial structural model. After three REMEDY cycles, R_{wp}, S, R_p, R_B and R_F significantly decreased to 4.44%, 1.20, 3.23%, 0.94% and 1.07%, respectively. The decreases in R indices demonstrate that the crystal structure can be seen more clearly from EDD instead of from the conventional structural parameters. In order to disclose the subtle EDD changes induced by MPF, we obtained the difference in EDD before and after the REMEDY cycles. The two-dimensional difference map at $y = 0$ showed two positive peaks with the heights of 0.006 and 0.0045 nm^{-3} (Fig. 3(a)). These peaks were located at 0.003 nm apart from the Al/Si2 site for the former and 0.002 nm apart from the Al/Si5 site for the latter. On the other hand, the residual electron densities were negligibly low at the O/C1 and O/C2 sites, indicating that the O and C atoms definitely occupy the same

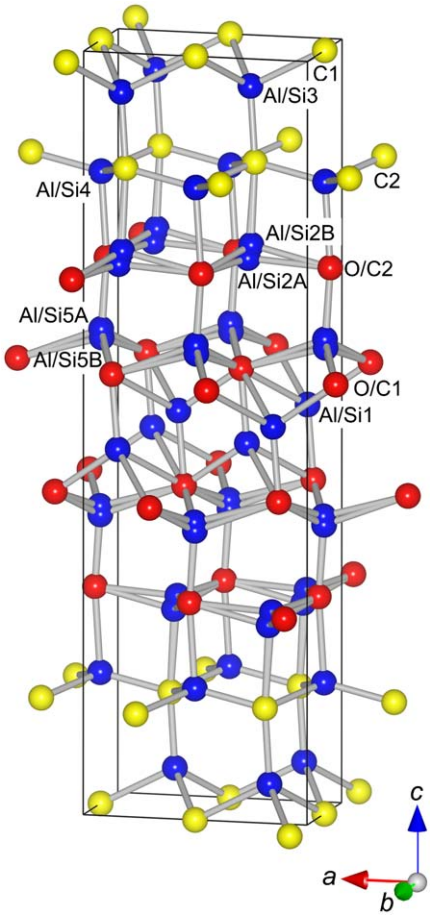

Fig. 4. Crystal structure of $[Al_{16.8}Si_{1.2}][O_{3.0}C_{11.0}]$. Space group $C2/m$.

sites in the crystal structure. These findings promoted us to build split-atom models for Al/Si2 and Al/Si5.

3.3. Split-atom model

In the split-atom model, each of the Al/Si2 and Al/Si5 sites at 4*i* was split into two independent crystallographic sites *M*A and *M*B (M = Al/Si2 and Al/Si5). We first refined the occupancies under the linear constrains of $g(MA)+g(MB)=1$ to find that all of the g parameters eventually converged to values very close to 0.5. Thus, we have fixed these parameters equal to 0.5 in successive least-

Table 1
Crystal data for $[Al_{16.8}Si_{1.2}][O_{3.0}C_{11.0}]$.

Chemical composition	$Al_{16.77(5)}Si_{1.23(5)}O_{3.04(9)}C_{10.96(9)}$
Space group	$C2/m$
a (nm)	0.57404(1)
b (nm)	0.331435(5)
c (nm)	1.92410(2)
β (deg)	90.036(1)
V (nm^3)	0.366076(9)
Z	1
D_x (mg m^{-3})	3.027

Table 2
Structural parameters for $[Al_{16.8}Si_{1.2}][O_{3.0}C_{11.0}]$[a]

Site	Wyckoff position	g	x	y	z	$100\times B$ (nm^2)
Al/Si1	4*i*	0.5	0.153(1)	0	0.5193(1)	0.13(7)
Al/Si2A	4*i*	0.5	0.157(2)	0	0.2768(2)	0.25(6)
Al/Si2B	4*i*	0.5	0.172(2)	0	0.2591(1)	0.25
Al/Si3	4*i*	1	0.168(1)	0	0.0512(1)	0.86(4)
Al/Si4	4*i*	1	0.5018(8)	0	0.17189(6)	0.80(3)
Al/Si5A	4*i*	0.5	0.502(2)	0	0.3784(2)	0.46(4)
Al/Si5B	4*i*	0.5	0.504(3)	0	0.3897(2)	0.46
C1	2*b*	1	0	1/2	0	0.72(7)
C2	4*i*	1	0.188(2)	0	0.1506(2)	0.72
O/C1	4*i*	1	0.127(1)	0	0.4215(1)	0.72
O/C2	4*i*	1	0.525(1)	0	0.2842(1)	0.72

[a] Site occupancies: O/C1: 48.6(14)% C and 51.4(14)% O; O/C2: 75.3(9)% C and 24.7(9)% O.

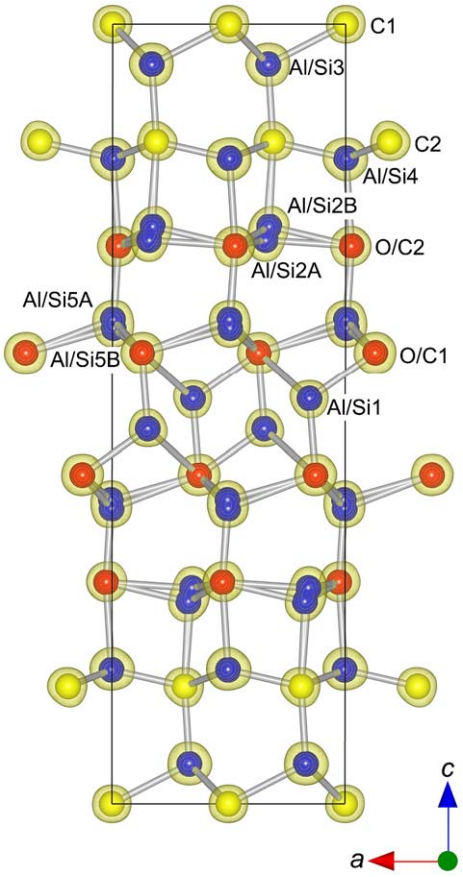

Fig. 6. Three-dimensional electron density distribution determined by MPF with the split-atom model viewed along the *b* axis. Isosurfaces expressed in wireframe style for an equidensity level of 0.002 nm^{-3}.

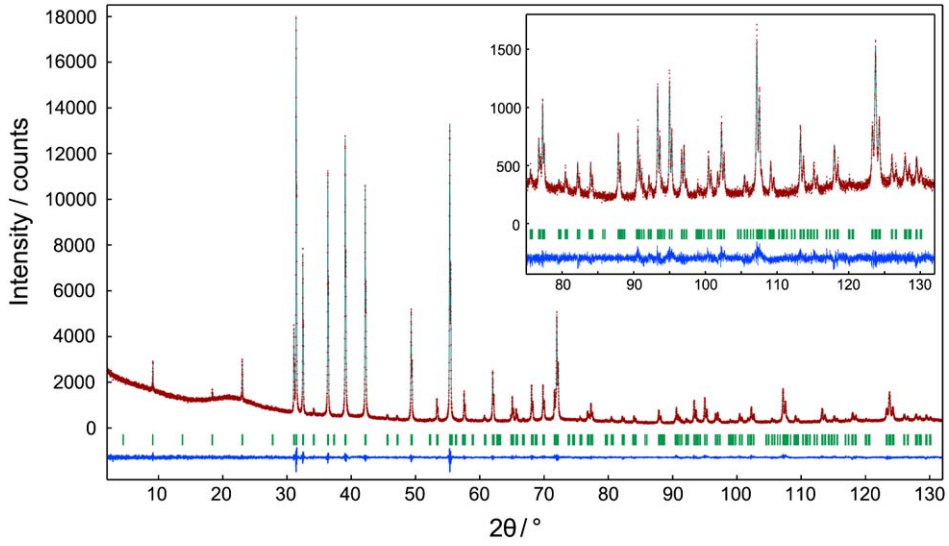

Fig. 5. Comparison of the observed diffraction pattern of $[Al_{16.8}Si_{1.2}][O_{3.0}C_{11.0}]$ (symbol: +) with the corresponding calculated pattern (upper solid line). The difference curve is shown in the lower part of the diagram. Vertical bars indicate the positions of Bragg reflections.

squares cycles. The parameters $B(MA)$ and $B(MB)$ were constrained to be equal to each other. The final Rietveld refinement resulted in satisfactory R indices of $R_{wp} = 4.45\%$ ($S = 1.21$), $R_p = 3.30\%$, $R_B = 3.47\%$ and $R_F = 2.53\%$, indicating that the disordered arrangements of Al/Si2 and Al/Si5 sites can be represented adequately with the split-atom model in Fig. 4. The individual separation distances are 0.035(1) nm for (Al/Si2A)–(Al/Si2B) and 0.022(1) nm for (Al/Si5A)–(Al/Si5B). Crystal data are given in Table 1, and the final atomic positional and B parameters are given in Table 2. The chemical composition was found to be $Al_{16.77(5)}Si_{1.23(5)}O_{3.04(9)}C_{10.96(9)}$, with the chemical formula of $[Al_{16.8}Si_{1.2}]_{\Sigma_{18}}[O_{3.0}C_{11.0}]_{\Sigma_{14}}$ (space group $C2/m$, $Z = 1$).

We used the MPF method again and subsequently obtained the difference in EDD before and after the REMEDY cycles to confirm the validity of the split-atom model. After two REMEDY cycles, R_{wp}, S, R_p, R_B and R_F further decreased to 4.20%, 1.14, 3.09%, 0.92% and 1.05%, respectively. The decreases in R indices indicate that the present disordered structure is better expressed with electron densities than with the structural parameters in Table 2. Observed, calculated and difference XRPD patterns for the final MPF are plotted in Fig. 5. The two-dimensional difference map at $y = 0$ (Fig. 3(b)) gave much lower residual electron densities, indicating that the EDD determined by the final MPF is explained sufficiently by the present split-atom model. For example, the three-dimensional electron-density images at the Al/Si2 and Al/Si5 sites (Fig. 6) show broadening, the equidensity isosurfaces of which are in reasonably good agreement with the atom arrangements. We therefore concluded that, as long as the crystal structure was expressed by a structural model, the present split-atom model would be satisfactory.

3.4. Structure description

The disordered structure can be regarded as a statistical average of the two twin-related structural configurations with the low-symmetry subgroup Cm (Fig. 7). When the two-fold axes parallel to [010] are removed from the space group $C2/m$, the resulting space group is Cm, with a center of symmetry being lost concomitantly. The two structural configurations as shown in Fig. 7 are therefore related not only by a pseudo-symmetry two-fold rotation but also by a pseudo-symmetry inversion. Thus,

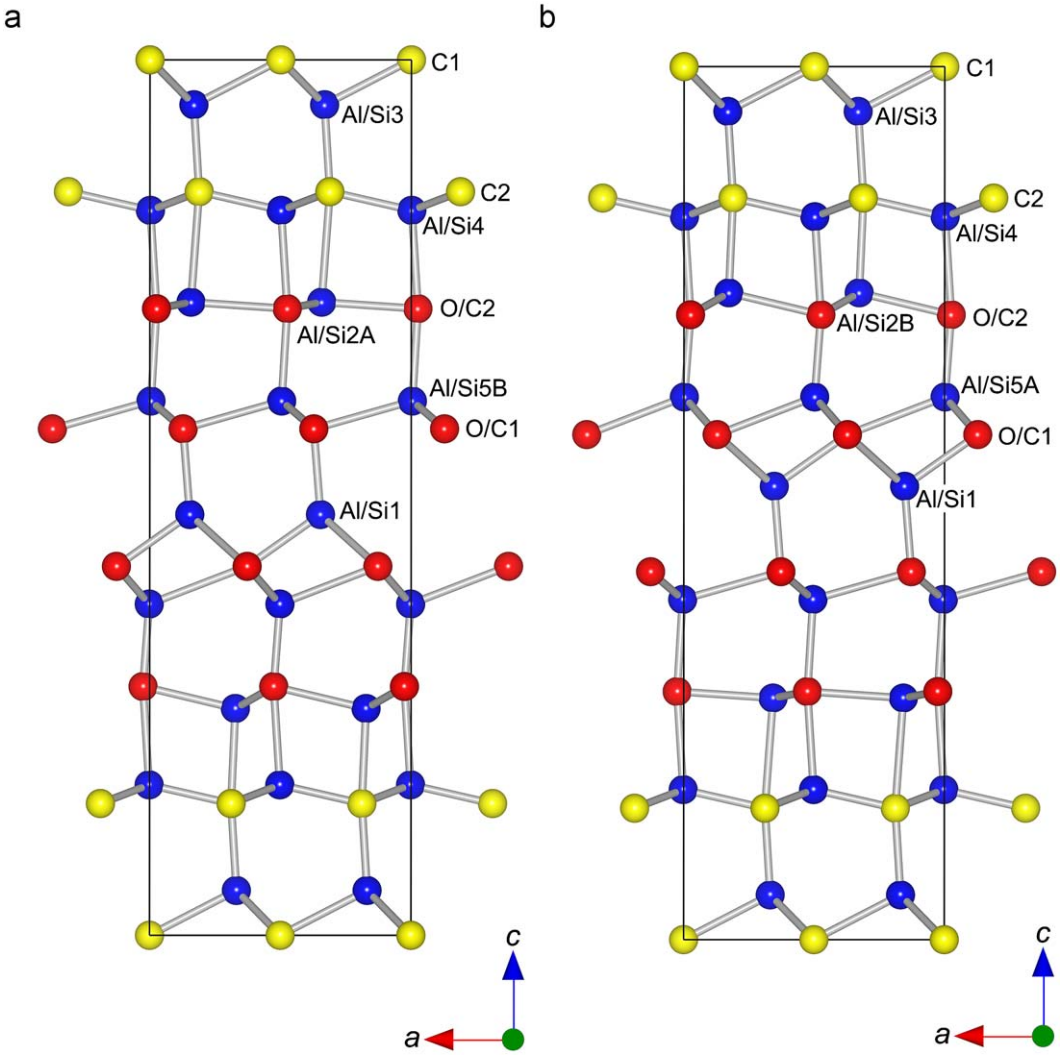

Fig. 7. Crystal structures of the two orientation states of $[Al_{16.8}Si_{1.2}][O_{3.0}C_{11.0}]$ viewed along the b axis. Space group Cm. The two structural configurations (a) and (b) are related by the pseudo-symmetry inversion.

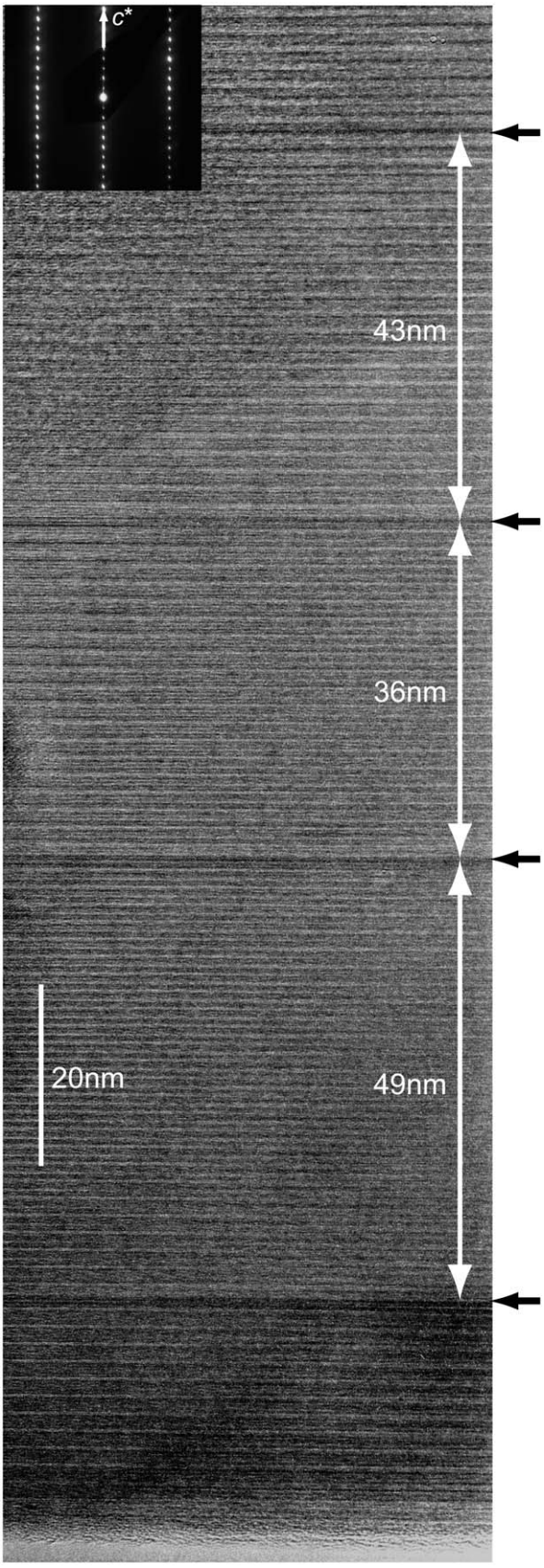

Fig. 8. Lattice image showing plane defects (indicated by arrows) perpendicular to [001]. The defects most probably correspond to the inversion twin boundaries.

the crystal must be an inversion twin. Actually, we observed using TEM the lattice defects parallel to (001), which must correspond to the inversion twin boundaries (Fig. 8). The distance between the adjacent boundaries (i.e., twin width) ranged from 36 to 49 nm with the average distance of 42.7 nm [(43+36+49)/3 = L]. Accordingly, the individual twin domains contained on the average about 22 ($=L/d_{(001)}$) unit cell along the direction perpendicular to (001). The dimensions of twin domains would be within the coherence range of X-rays, and hence the crystal structure has been satisfactorily represented by the split-atom model. One of the two orientational twin domain contained the Al/Si2A and Al/Si5B sites, and the other involved the Al/Si2B and Al/Si5A sites (Fig. 7). Because the occupancies of these sites as well as that of Al/Si1 site were all equal to 0.5, the actual domain ratio should be almost 0.5:0.5. This twin structure is most probably originated during crystal growth.

The atomic configurations are shown for $[Al_{16.8}Si_{1.2}][O_{3.0}C_{11.0}]$, Al_4C_3, Al_4SiC_4 and $Al_4Si_2C_5$ (Fig. 9). The crystal structure of $[Al_{16.8}Si_{1.2}][O_{3.0}C_{11.0}]$ can be regarded as a layered structure, which consists of *A*-type $[(Al,Si)_4(O,C)_4]$ unit layer and *B*-type $[(Al,Si)(O,C)_2]$ single layer with stacking sequence of $\langle ABA \rangle$ along the *c* axis. In Table 3, only (Al,Si)–(O,C) bonds belonging to one of the two twin-related orientations are reported, excluding possible bonds between atoms of different orientation states. The Al and Si atoms are tetrahedrally coordinated by O and/or C atoms with the mean (Al,Si)–(O,C) distance of 0.205 nm, which is comparable to the mean (Al,Si)–C distances of the $[(Al,Si)C_4]$ polyhedra in Al_4C_3 (0.206 nm), Al_4SiC_4 (0.202 nm) and $Al_4Si_2C_5$ (0.201 nm). Because the mean interatomic distance of $[Al_{16.8}Si_{1.2}][O_{3.0}C_{11.0}]$ compares well with those of Al_4C_3, Al_4SiC_4 and $Al_4Si_2C_5$, and also these structures are closely related to one another as shown in Fig. 9, $[Al_{16.8}Si_{1.2}][O_{3.0}C_{11.0}]$ can be regarded as, from a structural point of view, a carbide solid solution in which a relatively small amount of O atoms was dissolved into the C sites rather than an oxycarbide compound. The general formula of the solid solution is expressed by $[Al_{18-x}Si_x][O_yC_{14-y}]$, where *x*- and *y*-values are, respectively, 1.2 and 3.0 for the sample. One of the possible end member is Al_8SiC_7 ($x=2$ and $y=0$), which could be composed of a hexagonal layered structure with stacking sequence of $\langle ABA \rangle$.

A series of carbides in the Al_4C_3–SiC system can be represented by a general formula $Al_4C_3(SiC)_X$, where $X=0$ (Al_4C_3), 1/2 (Al_8SiC_7), 1 (Al_4SiC_4), 2 ($Al_4Si_2C_5$), 3 ($Al_4Si_3C_6$) and 4 ($Al_4Si_4C_7$). With $0 \le X \le 2$, the fraction of *A* layer (f_A) with respect to the *B* layer in the crystal structure steadily decreased with increasing *X*-value; the f_A- and *X*-values are well correlated by the equation $f_A = 1/(1+X)$. The f_A-values as predicted by this relationship are 0.25 for $Al_4Si_3C_6$ ($X=3$) and 0.2 for $Al_4Si_4C_7$ ($X=4$). Assuming that these crystal structures were also made up of the two types of layers *A* and *B*, the minimum stacking sequence would be *BABB* for $Al_4Si_3C_6$ and *BBABB* for $Al_4Si_4C_7$. These structures are comparable to those proposed by Oscroft et al. [1].

4. Conclusion

We have for the first time discovered a quaternary compound in the Al–Si–O–C system. The crystal structure was successfully determined from XRPD data and described in relation to those of the layered carbides Al_4C_3, Al_4SiC_4 and $Al_4Si_2C_5$. The compound was, from a structural point of view, regarded as a carbide solid solution rather than an oxycarbide compound. The crystal was most probably an inversion twin with an almost 0.5:0.5 domain ratio.

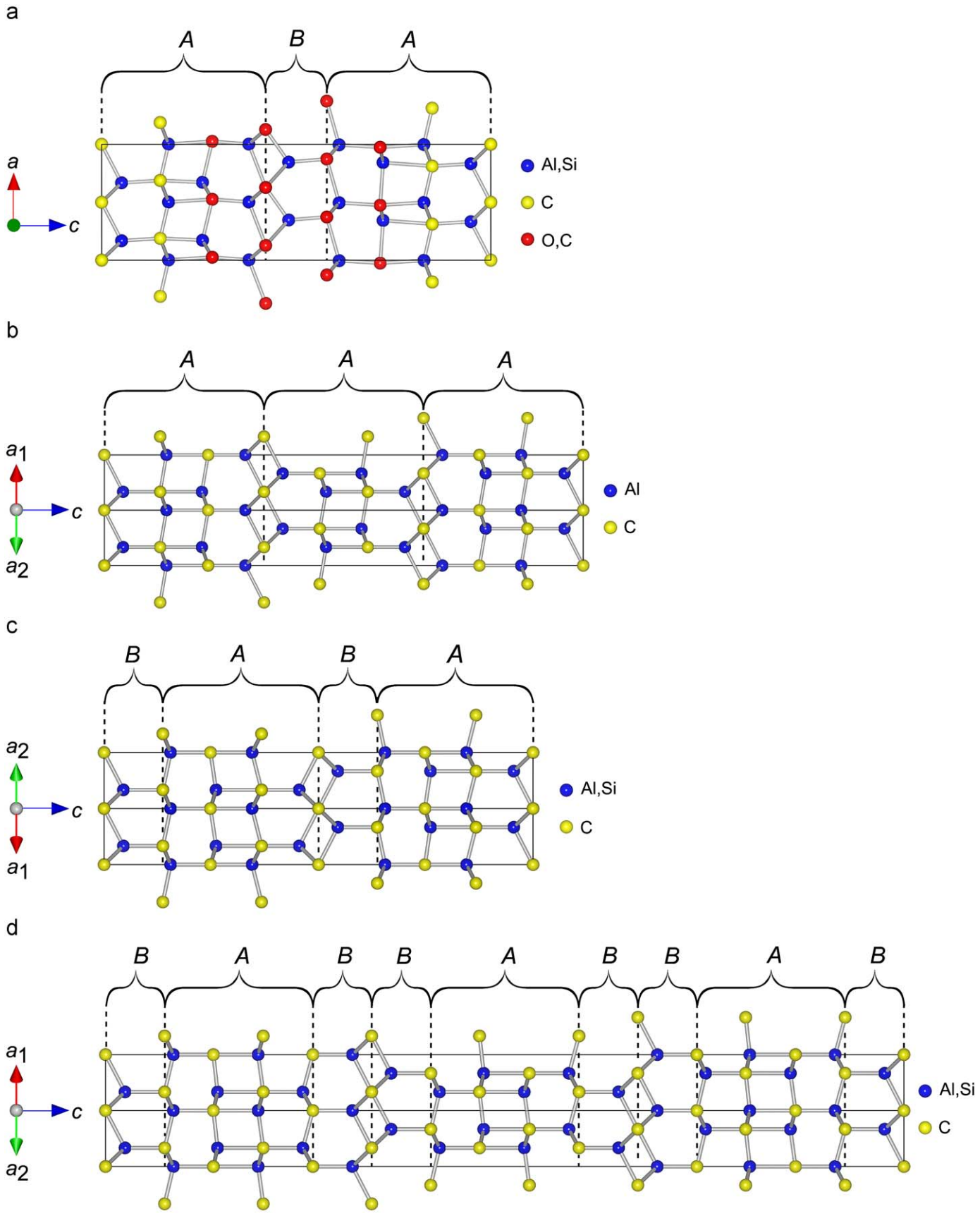

Fig. 9. Atomic configurations in (a) $[Al_{16.8}Si_{1.2}][O_{3.0}C_{11.0}]$, (b) Al_4C_3, (c) Al_4SiC_4 and (d) $Al_4Si_2C_5$, showing the crystal structures being made up of two types of layers *A* and *B*. The unit cells are represented by solid lines.

Table 3
Interatomic distances (nm) in $[Al_{16.8}Si_{1.2}][O_{3.0}C_{11.0}]$.

Al/Si1–O/C1	0.1889(4)
Al/Si1–O/C1	0.1973(8)
Al/Si1–O/C1	0.2373(5) × 2
〈Al/Si1–O/C〉	0.215
Al/Si2A–O/C2	0.1828(9) × 2
Al/Si2A–O/C2	0.212(2)
Al/Si2A–C2	0.2435(6)
〈Al/Si2A–O/C〉	0.205
Al/Si2B–O/C2	0.1921(7) × 2
Al/Si2B–O/C2	0.208(1)
Al/Si2B–C2	0.2091(7)
〈Al/Si2B–O/C〉	0.200
Al/Si3–C2	0.1914(5)
Al/Si3–C1	0.2147(5)
Al/Si3–C1	0.2155(3) × 2
〈Al/Si3–C〉	0.209
Al/Si4–C2	0.185(1)
Al/Si4–C2	0.2015(8) × 2
Al/Si4–O/C2	0.2165(4)
〈Al/Si4–O/C〉	0.201
Al/Si5A–O/C2	0.1817(6)
Al/Si5A–O/C1	0.1988(7) × 2
Al/Si5A–O/C1	0.230(2)
〈Al/Si5A–O/C〉	0.202
Al/Si5B–O/C1	0.1902(8) × 2
Al/Si5B–O/C2	0.2033(7)
Al/Si5B–O/C1	0.225(2)
〈Al/Si5B–O/C〉	0.202

Acknowledgments

Supported by a Grant-in-Aid for Scientific Research (no. 21360322) from the Japan Society for the Promotion of Science. Thanks are due to Mr. I. Yamaji, PANalytical Japan, Spectris Co. Ltd., for his technical assistance in XRPD.

Appendix A. Supplementary material

Supplementary data associated with this article can be found in the online version at doi:10.1016/j.jssc.2009.06.014.

References

[1] R.J. Oscroft, P. Korgul, D.P. Thompson, British Ceramic Proc. 42 (1989) 33–47.
[2] G.A. Jefeerey, V.Y. Wu, Acta Crystallogr. 20 (1966) 538–547.
[3] Th.M. Gesing, W. Jeitschko, Z. Naturforsch. 50b (1995) 196–200.
[4] V.J. Barczak, J. Am. Ceram. Soc. 44 (1961) 299.
[5] Z. Inoue, Y. Inomata, H. Tanaka, H. Kawabata, J. Mater. Sci. 15 (1980) 575–580.
[6] J. Schoennahl, B. Willer, M.J. Daire, Solid State Chem. 52 (1984) 163–173.
[7] B.L. Kidwell, L.L. Oden, R.A. McCune, J. Appl. Crystallogr. 17 (1984) 481–482.
[8] L.M. Foster, G. Long, M.S. Hunter, J. Am. Ceram. Soc. 39 (1956) 1–11.
[9] E.L. Amma, G.A. Jeffrey, J. Chem. Phys. 34 (1961) 252–259.
[10] V.E. Grass, Yu.I. Ryabkov, B.A. Goldin, P.A. Sitnikov, J. Struct. Chem. 45 (2004) 100–106.
[11] L.M. Foster, G. Long, M.S. Hunter, J. Am. Ceram. Soc. 39 (1956) 1–11.
[12] G.A. Jefeerey, M. Slaughter, Acta Crystallogr. 16 (1963) 177–184.
[13] A. Altomare, M.C. Burla, M. Camalli, B. Carrozzini, G.L. Cascarano, C. Giacovazzo, A. Guagliardi, A.G.G. Moliterni, G. Polidori, R. Rizzi, J. Appl. Crystallogr. 32 (1999) 339–340.
[14] H.M. Rietveld, J. Appl. Crystallogr. 2 (1969) 65–71.
[15] M. Takata, E. Nishibori, M. Sakata, Z. Kristallogr. 216 (2001) 71–86.
[16] F. Izumi, S. Kumazawa, T. Ikeda, W.-Z. Hu, A. Yamamoto, K. Oikawa, Mater. Sci. Forum 378–381 (2001) 59–64.
[17] L.M. Gelato, E. Parthé, J. Appl. Crystallogr. 20 (1987) 139–143.
[18] K. Momma, F. Izumi, J. Appl. Crystallogr. 41 (2008) 653–658.
[19] C. Dong, J. Appl. Crystallogr. 32 (1999) 838.
[20] P.E. Werner, L. Eriksson, M. Westdahl, J. Appl. Crystallogr. 18 (1985) 367–370.
[21] P.M. de Wolff, J. Appl. Crystallogr. 1 (1968) 108–113.
[22] G.S. Smith, R.L. Snyder, J. Appl. Crystallogr. 12 (1979) 60–65.
[23] A. Le Bail, H. Duroy, J.L. Fourquet, Mater. Res. Bull. 23 (1988) 447–452.
[24] F. Izumi, T. Ikeda, Mater. Sci. Forum 321–324 (2000) 198–203.
[25] R.A. Young, in: R.A. Young (Ed.), The Rietveld Method, Oxford University Press, Oxford, UK, 1993, pp. 1–38.
[26] H. Toraya, J. Appl. Crystallogr. 23 (1990) 485–491.